Wind-driven transport of thermospheric air parcels in the auroral zone

Mark Conde,[1] James H.Hecht,[2] Callum Anderson[1] [[1]Geophysical Institute, University of Alaska, [2]Aerospace Corporation]

Abstract

Data from ground-based optical instruments at Poker Flat and Fort Yukon in Alaska recorded during 2010 were used to examine the relationship between composition changes in the auroral thermosphere and transport effects by neutral winds. Thermospheric column [O]/[N_2] estimates were obtained from a pair of four-channel zenith-pointed narrow field photometers located at Poker Flat and Fort Yukon, whereas neutral winds at E and F-region heights were measured using an all-sky imaging Fabry-Perot spectrometer at Poker Flat. Wind fields were obtained over a spatial region around $1400\,\mathrm{km}$ in diameter in the F-region, or $700\,\mathrm{km}$ in the E-region, with a cadence of one observation every few minutes. We focus in particular on a sustained depletion of column [O]/[N_2] observed during the minor storm period of April 4-8, 2010. While various correlated events were noted, no systematic relation was found between between horizontal winds and the column [O]/[N_2] during this period (or indeed on any of the several tens of other days that we examined.) However during the storm there was a very obvious increase in activity of vertical winds, horizontal divergence, and associated wave activity. We suggest that the long-lived decrease in column [O]/[N_2] during the storm was due to vertical mixing being enhanced by a process akin to eddy diffusion. This is in contrast to the more typical picture of localized "upwellings" being driven by Joule heating, and then carrying molecular species aloft.

Introduction

A well known response of Earth's upper atmosphere to space weather disturbances at auroral latitudes is the reduction of [O]/[N_2] ratio in the middle and upper thermosphere following periods of strong geomagnetic forcing [e.g. *Craven et al.*, 1994; *Nicholas et al.*, 1997; *Immel et al.*, 1997; *Strickland et al.*, 1999; *Zhang et al.*, 2004; *Liou et al.,* 2005; *Immel et al.*, 2001, 2006; *Stephan et al.*, 2008]. These composition perturbations persist for many hours and undergo substantial transport by thermospheric winds. An example is shown in Figure 1. Unfortunately, there are very few simultaneous observations of thermospheric wind and composition during such storms. Thus, the objective of this study was to combine the Fabry-Perot and photometer data to determine whether any systematic transport effects could be discerned. The measurement geometry is indicated in Figure 2, which shows the locations of Poker Flat and Fort Yukon on a map of Alaska, together with an example two-dimensional horizontal wind field.

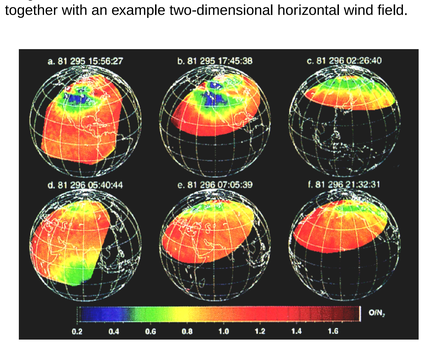

***Figure 1**: An example of [O]/[N_2] depletions, in this case observed by Strickland et al. [1999].*

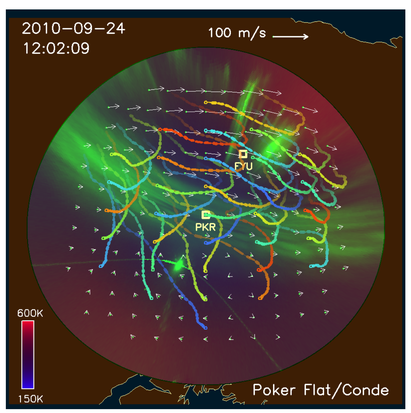

***Figure 2**: A map of Alaska, showing the horizontal wind field at E-region heights (white arrows) derived from all-sky Fabry-Perot spectrometer observations of the 558 nm emission. Background blue through red colors indicate the inferred Doppler temperature. The green background image shows an auroral arc observed in white light by the Poker Flat digital all-sky camera. Colored trails indicate the trajectories of "tracer particles" transported by this wind field.*

Instruments

The column [O]/[N_2] ratio was estimated from data recorded by photometers viewing the magnetic zeniths above Poker Flat and Fort Yukon in Alaska. Each is equipped with a four-position filter wheel, carrying filters tuned for the $427.8\,\mathrm{nm}$ emission from N_2^+, the $630.0\,\mathrm{nm}$ and $844.6\,\mathrm{nm}$ emissions from atomic oxygen, and the $871.0\,\mathrm{nm}$ emission from N_2. These instruments and associated analysis techniques have been described previously [e.g. *Hecht et al.*, 1995; 2006].

The all-sky Fabry-Perot has been described by *Conde & Smith* [1995, 1997, 1998] and *Conde et al.* [2001]. An all-sky lens maps a zenith-centered field of view spanning around 75° half-angle in the object space through an interference filter and etalon, with output optics then forming a sharp image onto a 512×512 pixel EMCCD camera. The etalon transmits around 6 interference orders. Techniques described by *Conde & Smith* [1997] are used to divide the field of view into 115 sub-regions, and to derive an independent spectrum from each such region. The spectra are fitted as described by *Conde* [2001] to produce line of sight winds. Horizontal vector wind fields are then obtained as described by *Conde & Smith* [1998].

Observations

We obtained several hundred nights of observations during 2009 through 2011; on a few tens of these all instruments were running properly, seeing conditions were good, and geomagnetic conditions were disturbed. We examined data from all of these, although here we focus on a 4-day period in early April 2010, during a minor geomagnetic storm. Figure 3 shows A_p and K_p indices that prevailed during this storm.

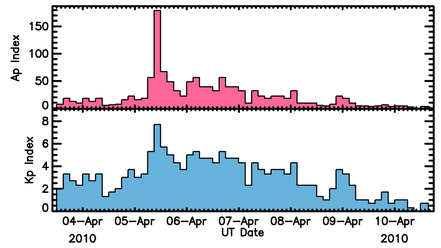

***Figure 3**: Time series plots of the planetary A and K magnetic indices over a 7-day period encompassing the 4 days chosen for study here.*

Figure 4 summarizes the observational data obtained on the four consecutive nights of April 4-7, 2010. The sixth panel down in these plots shows the column [O]/[N_2] values derived from the photometer measurements. It essentially indicates a factor by which the [O]/[N_2] ratio in MSIS must be multiplied in order to account for the observed brightnesses at the photometer's four wavelengths. This [O]/[N_2] factor was in the range 0.4 to 0.6 on April 4, when some aurora was observed but the associated magnetic perturbations were all less than $100\,\mathrm{nT}$. These pre-storm [O]/[N_2] values are typical of what was observed during many other periods with similar auroral and magnetic activity. The H-trace from the college magnetometer is shown in the bottom panels in Figure 4, which indicate that storm-level magnetic activity commenced at around $08{:}30$ UT on April 5, and continued at elevated but gradually declining levels for the next several days. The remaining panels in this figure show how the thermospheric winds, temperatures, and composition responded to this activity. The seventh and eighth panels down also show the response of the auroral energy flux and characteristic energy.

Temperatures and Horizontal Winds

The [O]/[N_2] response to the elevated magnetic activity is seen in the plots for April 5 to April 7. There was a clear drop in [O]/[N_2] following the onset of activity on April 5, down to values in the range 0.2 to 0.3. Generally reduced [O]/[N_2] values were also observed on the following two nights as well, at least during the dark portion of the observing period. (Higher values at the start and end of the observing period are due to dusk & dawn twilight affecting the optical measurements, and should be ignored.) The reduced [O]/[N_2] values observed over these 3 days are qualitatively consistent with previous observations of storm-time depleted [O]/[N_2] patches, similar for example to the data shown in Figure 1.

It is worth noting that the [O]/[N_2] response was very similar at Poker Flat and Fort Yukon. This was not always true, especially when aurora was occurring above one site but not the other.

Panels 2 and 3 of the plots in Figure 4 indicate substantial horizontal wind responses occurred during the period of elevated magnetic activity, especially in the F-region on April 5, when the geomagnetic zonal wind actually went off-scale on these plots. However, no systematic correlation was apparent between [O]/[N_2] and either component of horizontal wind, at either E or F-region heights. This was also true on other days that we studied. On a number of occasions we did see wind features coincident with [O]/[N_2] responses that likely were related, but we did not discern any systematic repeatable pattern to such events.

Panel 9 of the plots shows that there were also obvious temperature responses. F-region temperatures increased by as much as $200\,\mathrm{K}$ within 2 to 3 hours of activity starting, and remained high throughout the observing period. E-region temperatures (derived from the $557.7\,\mathrm{nm}$ emission) also responded to the geomagnetic activity, but not with the simple sustained heating seen in the F-region. Rather, the Doppler temperature became rather variable, which is the result of the $557.7\,\mathrm{nm}$ emission height changing in response to temporal and spatial variability in the characteristic energy of the auroral precipitation. But once again, we did not find any systematic relationship between [O]/[N_2] perturbations and the $557.7\,\mathrm{nm}$ or $630.0\,\mathrm{nm}$ Doppler temperatures.

Vertical Winds and Horizontal Divergence

The widely accepted mechanism for [O]/[N_2] depletions like those in Figure 1 is that storms produce high levels of Joule heating, which in turn drives upward winds that carry molecular species like N_2 into the middle and upper thermosphere. This displaces atomic oxygen, and results in a net lowering of the [O]/[N_2] ratio. Occurrence of this mechanism has been confirmed by the DE2 satellite (Figure 5 for example) and by many modeling studies [e.g. *Burns et al.*, 1991, 2006; *Rishbeth & Muller-Wodarg*, 1999]. However, it has proven remarkably difficult to observe this process in action from the ground. Presumably this is partly because localized regions of upwelling are far more likely to be encountered by a moving satellite that by an observatory at one fixed location. But equally important is that events similar to that in Figure 5 are actually quite rare, even in the DE2 data – they were encountered in probably less than one percent of the orbits.

Figure 4 suggests an alternate mechanism for generating [O]/[N_2] depletions, and *one that potentially occurs far more easily and frequently*. The top panel in these figures shows vertical wind, and the fourth panel down shows horizontal divergence. It is apparent by inspection that large oscillations began in both parameters immediately after the onset of magnetic activity, and these oscillations continued at least for the next two days. Separate analysis (not shown here) indicated that the neutral temperature in individual viewing directions also experienced similar oscillations. (Temperature oscillations are not apparent in the bottom panel of Figure 4 partly because of the plot scale, but also because these figures show all-sky median temperature, which does not resolve the fluctuations occurring at individual locations.) A second imaging Fabry-Perot located at Gakona (several hundred km south of Poker) saw the same oscillations in each of these parameters.

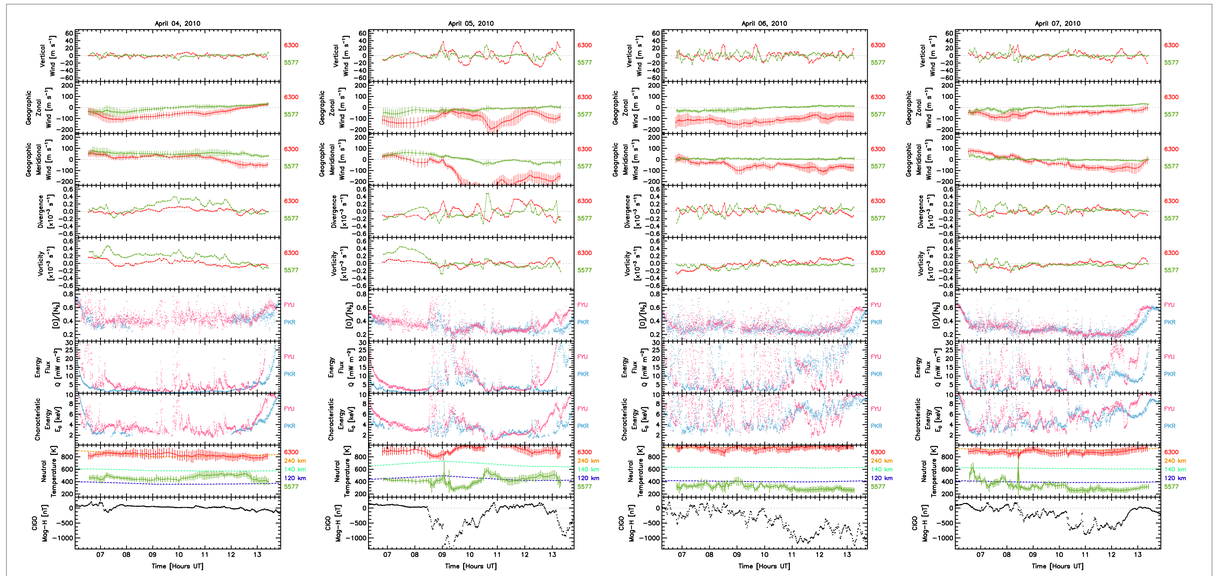

***Figure 4**: Panels from top to bottom show vertical wind, geographic zonal wind, geographic meridional wind, divergence, vorticity, column [O]/[N_2] ratio, auroral energy flux, auroral characteristic energy, neutral temperature, and the magnetometer H-component recorded at College, Alaska. Colors are used as follows – Red: Fabry-Perot $630\,\mathrm{nm}$ data; green: Fabry-Perot $558\,\mathrm{nm}$ data; light blue: photometer data from Poker Flat; pink: photometer data from Fort Yukon. The second-bottom panel also shows MSIS temperatures at various heights, calculated for the prevailing conditions.*

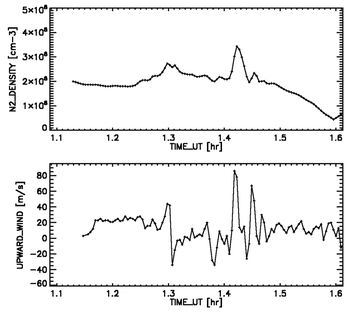

***Figure 5**: Data from the Dynamics Explorer 2 satellite recorded on day 322 of 1982. The top panel shows the number density of molecular nitrogen, projected to a fixed height of $300\,\mathrm{km}$. The bottom panel shows vertical wind. Enhanced N_2 densities observed at around 1.45 hours UT were collocated with a region of upward wind, which was presumably responsible for carrying the molecules aloft.*

These data indicate that the magnetic storm drove a complex field of small scale vertical wind oscillations. Further, the amplitude and phase relations between vertical wind, horizontal divergence, and temperature provide compelling evidence that these oscillations were due to thermospheric gravity waves. We therefore suggest here that the [O]/[N_2] reductions observed by the photometers at Poker and Fort Yukon were due to *enhanced vertical mixing resulting from the propagation and dissipation of thermospheric gravity waves induced by the storm*. This mechanism is quite different to the picture of discrete regions of upwelling carrying N_2 aloft in a single journey. Here the action occurs over many cycles of upward and downward motion, as gravity waves propagate and dissipate in the lower and middle thermosphere. The proposed mechanism is more akin to eddy diffusion than simple advection. It does not require especially intense regions of localized heating, and could instead potentially occur over a wide geographic area.

Conclusions

Measurements of thermospheric [O]/[N_2] column density ratio have been compared to imaging Fabry-Perot observations of neutral wind and temperature at both E and F-region heights during a 4-day storm period in April 2010. The observations showed that:

- The [O]/[N_2] column ratio decreased immediately after the onset of magnetic activity, and remained low for several days.
- Significant perturbations to neutral winds and temperatures also began occurring immediately after the storm onset.
- We did not find any obvious association between horizontal winds and [O]/[N_2] perturbations during the storm period that would indicate horizontal transport driving composition changes.
- Examination of additional data (not shown here) also failed to show any evidence of a repeatable signature of composition being driven by horizontal transport. These data do not rule out such effects; it's more likely that the responses were too complex and variable to be immediately apparent.
- However, we did see obvious evidence of large amplitude thermospheric gravity waves established in response to the magnetic activity.
- We propose here that the observed reductions in [O]/[N_2] were due to enhanced vertical mixing occurring as these waves propagated and dissipated in the thermosphere. This process would be more diffusive than advective in character, and could easily occur over large geographic areas without any special constraints on the original driver processes.

References

Burns, A. G., T. L. Killeen, and R. G. Roble (1991), A Theoretical Study of Thermospheric Composition Perturbations During an Impulsive Geomagnetic Storm, *J. Geophys. Res.*, 96(A8), 14,153–14,167, doi:10.1029/91JA00678.

Burns, A. G., W. Wang, T. L. Killeen, S. C. Solomon, and M. Wiltberger (2006), Vertical variations in the N2 mass mixing ratio during a thermospheric storm that have been simulated using a coupled magnetosphere-ionosphere-thermosphere model, *J. Geophys. Res.*, 111, A11309, doi:10.1029/2006JA011746.

Conde, M. and R. Smith (1997), Phase compensation of a separation scanned, all-sky imaging Fabry-Pérot spectrometer for auroral studies, *Appl. Opt.*, 36, 5441-5450.

Conde, M., and R. W. Smith (1998), Spatial structure in the thermospheric horizontal wind above Poker Flat, Alaska, during solar minimum, *Journal of Geophysical Research*, 103, 9449-9471.

Conde, M., Analysis of Fabry-Perot spectra of lidar backscatter echoes Morris, R.J., Wilkinson, P.J. (ed.) *ANARE Reports* No. 146. 91–114, 2001.

Conde, Craven, Immel, Hoch, Stenbaek-Nielsen, Hallinan, Smith, Olson, Wei Sun, Frank, and Sigwarth, (2001), Assimilated observations of thermospheric winds, the aurora, and ionospheric currents over Alaska, *J. Geophys. Res.* 106:10493-10508.

Craven, J. D., A. C. Nicholas, L. A. Frank, D. J. Strickland, and T. J. Immel (1994), Variations in the FUV dayglow after intense auroral activity, *Geophys. Res. Lett.*, 21(25), 2793–2796, doi:10.1029/94GL02458.

Hecht, J. H., A. B. Christensen, D. J. Gutierrez, D. C. Kayser, W. E. Sharp, J. R. Sharber, J. D. Winningham, R. A. Frahm, D. J. Strickland, and D. J. McEwen (1995), Observations of the Neutral Atmosphere Between 100 and 200 km Using ARIA Rocket-Borne and Ground-Based Instruments, *J. Geophys. Res.*, 100(A9), 17,285–17,298, doi:10.1029/95JA00229.

Hecht J.H., D.J. Strickland, and M.G. Conde (2006), The Application of Ground-based Optical Techniques for Inferring Electron Energy Deposition and Composition Change during Auroral Precipitation Events, *Journal of Atmospheric and Solar Terrestrial Physics* 68:1502-1519.

Immel, T. J., J. D. Craven, and L. A. Frank (1997), Influence of IMF B/sub y/ on large-scale decreases of O column density at middle latitudes, *J. Atmos. Sol-Terr. Phys.*, 59, 725-737.

Immel, T., G. Crowley, J. Craven, and R. Roble (2001), Dayside enhancements of thermospheric O/N2 following magnetic storm onset, *J. Geophys. Res.*, 106(A8), 15471-15488.

Immel, T. J., G. Crowley, C. L. Hackert, J. D. Craven, and R. G. Roble (2006), Effect of IMF By on thermospheric composition at high and middle latitudes: 2. Data comparisons, *J. Geophys. Res.*, 111, A10312, doi:10.1029/2005JA011372.

Liou, K., P. T. Newell, B. J. Anderson, L. Zanetti, and C.-I. Meng (2005), Neutral composition effects on ionospheric storms at middle and low latitudes, *J. Geophys. Res.*, 110, A05309, doi:10.1029/2004JA010840.

Nicholas, A. C., J. D. Craven, and L. A. Frank (1997), A survey of large-scale variations in thermospheric oxygen column density with magnetic activity as inferred from observations of the FUV dayglow, *J. Geophys. Res*, 102, 4493-4510.

Rishbeth, H and I. C. F. Müller-Wodarg (1999), Vertical circulation and thermospheric composition: a modelling study, Annales Geophysicae Vol 17, Number 6, 794-805, DOI: 10.1007/s00585-999-0794-x.

Stephan , A. W., R. R. Meier, and L. J. Paxton (2008), Comparison of Global Ultraviolet Imager limb and disk observations of column O/N2 during a geomagnetic storm, *J. Geophys. Res.*, 113, A01301, doi:10.1029/2007JA012599.

Strickland, D. J., R. J. Cox, R. R. Meier, and D. P. Drob (1999), Global O/N2 derived from DE 1 FUV dayglow data: Technique and examples from two storm periods, *J. Geophys. Res.*, 104, 4251-4266.

Zhang, Y., L. J. Paxton, D. Morrison, B. Wolven, H. Kil, C.-I. Meng, S. B. Mende, and T. J. Immel (2004), O/N2 changes during 1–4 October 2002 storms: IMAGE SI-13 and TIMED/GUVI observations, *J. Geophys. Res.*, 109, A10308, doi:10.1029/2004JA010441.